ACS Sustainable Chemistry & Engineering

pubs.acs.org/journal/ascecg

Research Article

Fundamentals of Hybrid Cellulose Nanofibril Foam Production by Microwave-Assisted Thawing/Drying Mechanism

Md Musfiqur Rahman, Islam Hafez,* Mehdi Tajvidi, and Aria Amirbahman

Cite This: *ACS Sustainable Chem. Eng.* 2023, 11, 13240−13250

Read Online

ACCESS | Metrics & More | Article Recommendations | Supporting Information

ABSTRACT: Cellulose nanofibril (CNF) porous structures (foams/aerogels) are typically produced using energy-intensive processes such as freeze drying. In this study, a novel microwave-assisted thawing process was developed to produce low-density (36 kg/m^3) CNF foams. The process involved the freezing of CNF and urea suspension followed by immediate thawing in the microwave. A slow freezing rate produced a uniform pore structure, whereas fast freezing using liquid nitrogen resulted in the aggregation of CNF upon thawing. The in-situ carbamate crosslinking resulted from the addition of urea provided wet stability and was confirmed by FTIR and nitrogen content analysis. The compressive properties of the foams were evaluated in both dry and wet conditions. In addition, iron oxide nanoparticles were used to assess the feasibility of producing hybrid foams via this novel method. This innovative and energy-efficient approach to produce foams from cellulosic nanomaterials has the potential to be scaled up and is expected to promote the use of renewable nanomaterials in a wider range of applications.

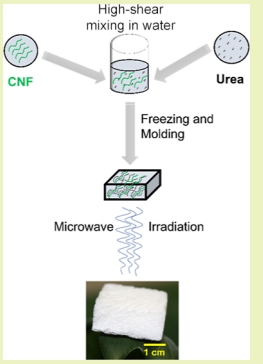

KEYWORDS: *cellulose nanofibrils, urea, foam, microwave, wet stability, crosslinking*

Downloaded via VIRGINIA POLYTECH INST STATE UNIV on May 6, 2024 at 19:31:25 (UTC).
See https://pubs.acs.org/sharingguidelines for options on how to legitimately share published articles.

INTRODUCTION

Cellulosic-based materials have been receiving interest from a wide range of fields because of their distinctive attributes, particularly chemical inertness, exceptional mechanical properties, vast abundance, biodegradability, scope for chemical modification, and low thermal expansion coefficient.[1−3] For example, the interest in cellulose-based packaging materials is continually rising as researchers have been attempting to replace petroleum-based plastics with goods manufactured from renewable materials.[4−6] Other applications included recyclable composites,[7] energy storage,[8] biological applications,[9] nutritional additives,[10] and water treatment.[11]

While many forms of cellulose nanomaterials do exist, cellulose nanofibrils (CNFs) are a major type that are prepared by mechanical refining or other mechanical size reduction techniques.[1] CNF-based foams are excellent alternatives to those made of petroleum-based materials.[12] Due to the low thermal conductivity of CNF-based foams, there is a tremendous potential for their application in insulation[13] and the replacement of petroleum-based materials. Additionally, these foams and aerogels have been effectively used to filter contaminated water.[14−17]

Freeze drying and supercritical drying are common methods to produce low-density 3D structures from CNFs.[18] However, these processes are lengthy and complex, rendering them unattractive options to the industrial sector. Additionally, chemical modifications are oftentimes needed to overcome the inherent hydrophilicity of cellulosic materials. Other researchers have attempted to produce CNF-based foams using oven drying and foaming agents.[19,20] A recent study reported the application of freeze−thawing−drying cycles in the presence of urea[21] to produce low-density structures from microfibrillated cellulose (MFC)—another term often used in lieu of CNF, using a combination of oven and air drying. An MFC to urea ratio of 1:1 was needed for producing the MFC foams with the least shrinkage and deformation. In addition, those MFC foams showed higher compressive properties compared to freeze-dried foams. However, the overall drying step was still time-consuming and somewhat comparable with freeze-drying and supercritical CO_2 drying.

Urea has been extensively utilized to improve the solubility of cellulose in aqueous NaOH or LiOH solutions. To explain the urea−NaOH−water system, Cai and Zhang[22] proposed a mechanism where the dissolution of cellulose in LiOH/urea and NaOH/urea was achieved at low temperature through the formation of a coating layer of urea hydrate around individual fibrils governed by hydrogen bonding donor−acceptor interaction that prevented aggregation. A similar concept was utilized by Fauziyah et al.[23] to make crosslinked cellulose aerogels from coir fibers. Despite the contributions of previous researchers in explaining such a system, the interaction

Received: January 31, 2023
Revised: August 3, 2023
Published: August 30, 2023

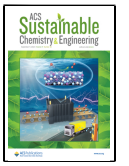

ACS Publications

© 2023 American Chemical Society

Scheme 1. Schematic Diagram of UCNF and UCNF-IONP Foam Forming Procedure

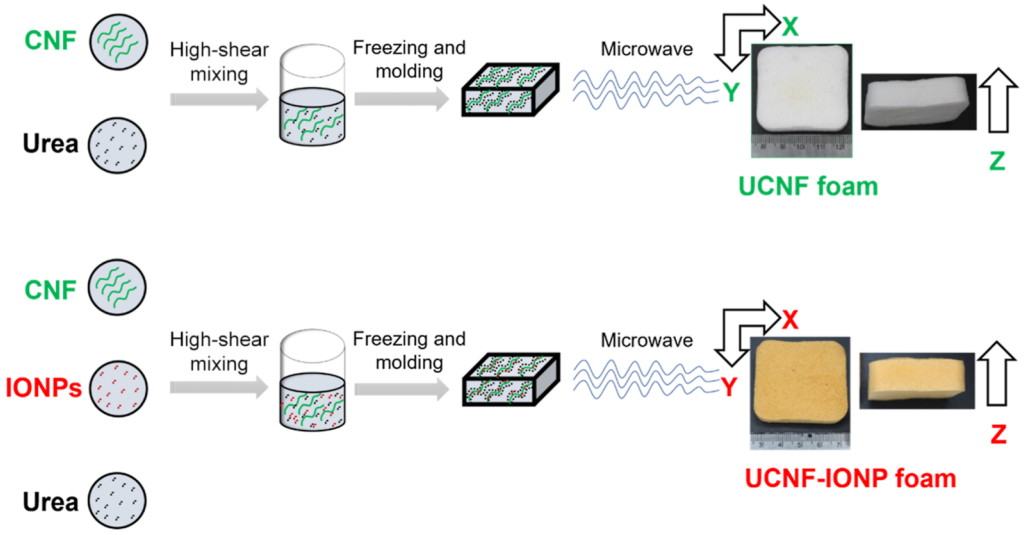

mechanism between cellulose and urea to form foam structures requires further investigations.

A non-conventional technique to produce foams from lignocellulosic materials using microwave (MW) drying has been recently reported.[24,25] In these studies, low-density foams from thermomechanical pulp fibers and wood sawdust were prepared using microwave drying, and CNFs were added as a binder. Compared to convection/oven drying, this method is considerably faster and more energy-efficient.[26,27] During microwaving, heat is generated when a dielectric material with induced or permanent dipoles is subjected to microwave radiation. According to the literature, two mechanisms—dipolar polarization and ionic conduction—underlie microwave heating, while a third, known as interfacial polarization, combines the two.[28,29]

Hybrid foams are currently gaining a great interest due to their multifunctionality. Previous studies have addressed the potential of nanoparticle-incorporated CNF foams and their applications in fields such as fire retardant,[30] energy storage,[31] and contaminant removal from water.[32] The lack of efficient drying techniques is a significant contributor to the high cost and energy consumption of the manufacturing process of such hybrid CNF foams. In our recent work,[16] we produced a freeze-dried iron-oxide-incorporated CNF aerogel that showed promising results for arsenic removal from water. However, the preparation of these low-density hybrid CNF aerogels is costly and time-consuming. Therefore, presenting a proof-of-concept for the potential of other energy-efficient methods to produce hybrid foams will be valuable for a wide range of applications.

This study highlighted a novel process of making foams from CNF based on an immediate thawing protocol of frozen CNF suspension that was not previously reported. The study also provided an in-depth understanding of the immediate thawing process and the chemical and physical interactions between CNF, urea, and water. In addition, the mechanism of foam formation using a microwave system was investigated. The obtained foams were characterized, and the feasibility of forming hybrid foams from CNF and iron oxide nanoparticles (IONPs) was examined.

EXPERIMENTAL SECTION

Materials. CNFs were provided by the University of Maine Process Development Center (PDC) (Orono, ME). The mechanically refined bleached softwood kraft pulp was used to produce 90% fine content (percentage of fibers with a length of <200 μm) at a consistency of 3 wt % CNF. Urea (NH_2CONH_2; 99.0−100.5%) was purchased from Sigma-Aldrich (St. Louis, MO, USA). Polycup (polyamide-epichlorohydrin) 5150 crosslinker (26 wt %) was supplied by Solenis (Wilmington, DE, USA). All reagents were obtained as analytical grade and used without further purification.

Foam Preparation. Urea contents from 5 to 50 wt % were selected based on the total dry mass of CNF. The desired amount of urea was added as an aqueous solution to dilute the 3 wt % CNF suspension to 2 wt %, followed by a high-shear mixing using an electric stirrer mixer (JJ-1 Precise Power Mixer, Hangzhou Feng Hai Electronic Commerce Co., Ltd., Zhejiang, China) for 5 min. In a rectangular plastic mold (5.23 × 5.23 × 1.82 cm), 40 g of CNF-urea suspension (UCNF) was placed. To control the freezing rate, the freezing chamber of a Harvest Right freeze-dryer (North Salt Lake, UT, USA) was used (no vacuum was applied). The UCNF suspensions were placed in the freezing chamber initially at 2 °C, and three freezing rates (0.06, 0.39, and 1.78 °C/min) were used to lower the temperature to −20 °C. Freezing with liquid nitrogen (flash freezing) was also conducted. Finally, all the frozen samples were stored in a freezer at −20 °C prior to the subsequent step.

The frozen UCNF suspensions were removed from the mold and placed on a paper towel in an LG LMC1575 microwave oven (LG Electronics Inc., Seoul, South Korea). The microwave oven has the option of customizing the power input (up to 1200 W) at 10% intervals using a built-in smart inverter. The drying procedure is composed of two stages. First, 1200 W of energy was applied for 3 min. Then, a total of 4 min of heating at 360 W was applied with 1 min intervals between every minute of heating to avoid over-drying. The final moisture content after microwaving was ∼7−10%. Drying beyond a 7% moisture content resulted in shrinkage and warpage of the samples. To avoid this, the samples were kept at room temperature overnight to further reduce the moisture content. Finally, the foams were conditioned at a relative humidity of 50 ± 2% and a temperature of 23 ± 2 °C for 24 h before further testing.

Hybrid foams were prepared by adding various amounts of IONPs (3, 5, 7, and 10 wt % based on the dry mass of CNF) to the CNF and urea mixture. The preparation of IONPs was described by Rahman et al. (2021)[16] and used herein to demonstrate the feasibility of preparing hybrid foams using our microwave-assisted thawing/drying method. Scheme 1 schematically illustrates the UCNF foam-forming procedure.

https://doi.org/10.1021/acssuschemeng.3c00599
ACS Sustainable Chem. Eng. 2023, 11, 13240−13250

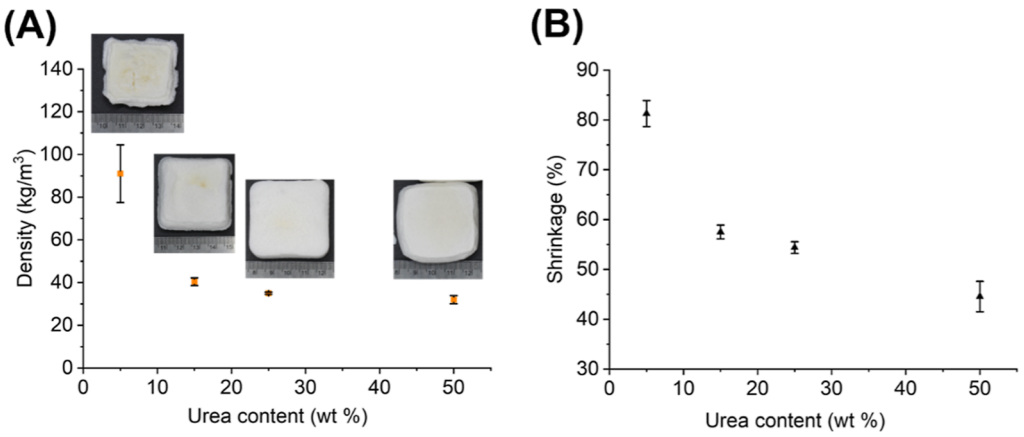

Figure 1. Change in density (A) and volumetric shrinkage (B) of the UCNF foams with respect to urea content. The error bars represent one standard deviation among three replicates. The digital photograph of each sample is shown on the corresponding density plot.

Freeze-dried foams were prepared for comparison purposes. To this end, two different batches of 2 wt % CNF were prepared with and without a Polycup crosslinker (5 wt % of the total dry mass of CNFs). The CNFs with a crosslinker were stirred with a magnetic stirrer for 5 min to ensure the homogeneous mixing of the crosslinker. Finally, the suspensions were poured into the rectangular molds to freeze dry in a Harvest Right freeze-dryer (North Salt Lake, UT, USA). The temperature cycles of the freeze dryer were −34.4, −6.7, 4.4, 15.6, and 32.2 °C for 8, 10, 8, 3, and 3 h, respectively. The CNF samples with a crosslinker were cured in a vacuum oven for 3 h at 105 °C to induce crosslinking.

Foam Characterization. The morphology of the foams was examined using a Zeiss NVision 40 scanning electron microscope (Carl Zeiss AG, Oberkochen, Germany). The foam specimen was sliced (2−4 mm thick) with a sharp blade and placed on a sample stub using a double-sided carbon tape. All the samples were sputter coated with a 10 nm layer of gold-palladium, and an electron high tension voltage of 3 kV was maintained at the time of scanning.

Optical microscopy was performed using an Olympus SZX16 dissecting microscope (Olympus Corporation, Shinjuku-ku, Tokyo, Japan) fitted with a Zeiss Axiocam Erc 5s (Carl Zeiss AG, Oberkochen, Germany). The *X*−*Y* and *Z*-directional cross sections of the UCNF foams were sliced using a sharp blade while maintaining 2−4 mm of thickness.

The nitrogen content of the UCNF foams was measured by a Leco TruMac CN928 Carbon/Nitrogen analyzer (Leco Corporation, St. Joseph, MI, USA) using the combustion method. Leco orchard leaves were used as a certified reference material with a N content of 2.31 ± 0.05%. Three replicates of each type were used to calculate an average.

The mass loss experiments for both UCNF and UCNF-IONP hybrid foams in water were conducted by agitating the foams at 125 rpm for 48 h, followed by drying in a convection oven at 80 °C for 6 h. The mass loss (%) was calculated gravimetrically by comparing the dry weights of the initial and post-dried foams.

A Spectrum Two FTIR spectrophotometer (PerkinElmer, Waltham, MA, USA) was used to examine chemical interactions between CNF and urea. Additionally, one of the UCNF foam samples was rinsed thoroughly with 2 L of water to remove residual urea and subsequently dried in a convection oven for 6 h at 80 °C. The spectra were normalized with respect to the wavenumber 1055 cm^{-1} that represents the stretching vibration of the cellulose backbone not altered by any reaction.[33]

To further evaluate the chemical properties of the foams, ^{13}C solid-state NMR was performed using a Neo 600 MHz system (Bruker Corporation, Billerica, MA, USA) equipped with a high-resolution magic-angle spinning (HRMAS) probe operated at 10,000 Hz. Foam samples were cut into 1 × 3 mm pieces weighing ∼30 mg and firmly packed into a 50 μL rotor. One-dimensional (1D) ^{13}C spectra of each sample were collected with 720 scans (1 h), which were repeated 17 times (total 18 spectra per sample). The spectra of each sample were processed, referenced to the ^{13}C spectrum of the glucose standard, and summed as the final ^{13}C spectrum with Mnova 14 software (Mestrelab Research, S.L., A Coruña, Spain).

Additional experimental details are available in the Supporting Information.

RESULTS AND DISCUSSION

Factors Influencing the Formation of Porous Foam Structures. Figure 1A,B shows the change in foam density and volumetric shrinkage as a function of urea content. Foams prepared with 5 wt % urea content had the highest density (91 kg/m^3) and maximum shrinkage. There is no statistical difference in densities among samples prepared with 15, 25, and 50 wt % urea (32−40 kg/m^3). With respect to shrinkage, there is no statistical difference in volumetric shrinkage values of foams containing 15 and 25 wt % urea. However, freeze-dried foams prepared from CNF at a similar consistency showed statistically lower density (25 ± 0.6 kg/m^3) and shrinkage (21 ± 2%) values compared to the UCNF foams prepared through microwave irradiation. Although there was no statistical difference in densities between 15 and 25 wt % UCNF foams, foams with 25 wt % urea were used for the rest of the experiments due to the uniformity of their shape. This urea wt % is lower than that used in the previously published studies,[21,34] where a 1:1 CNF urea ratio was needed to obtain a foamed structure via a freeze−thawing process followed by oven and air drying. The porosity of the UCNF foams with 25 wt % urea content was 97−98%. These foams were prepared through instantaneous microwave thawing, which means that the frozen samples were immediately placed in the microwave for thawing and drying. The effect of thawing conditions will be discussed further in later sections.

Scanning electron microscopy (SEM) images of foam samples with and without urea are shown in Figure 2A. It is evident that CNF without urea did not produce any foam structure. Starting from 15 wt %, the open cell pores became more visible. The foams prepared with 25 and 50 wt % urea content also showed similar pore structures; however, an increase in the urea content resulted in a decrease in the loosely hanging fibrils that may be due to the hydrogen bonding of residual urea with CNF surface[35] or the higher extent of crosslinking, which will be discussed in a later section. The pores structure of freeze-dried foams without the addition of urea was nearly similar to that of the UCNF foams (Figure 2B) at similar densities. However, the presence of loosely

https://doi.org/10.1021/acssuschemeng.3c00599
ACS Sustainable Chem. Eng. 2023, 11, 13240−13250

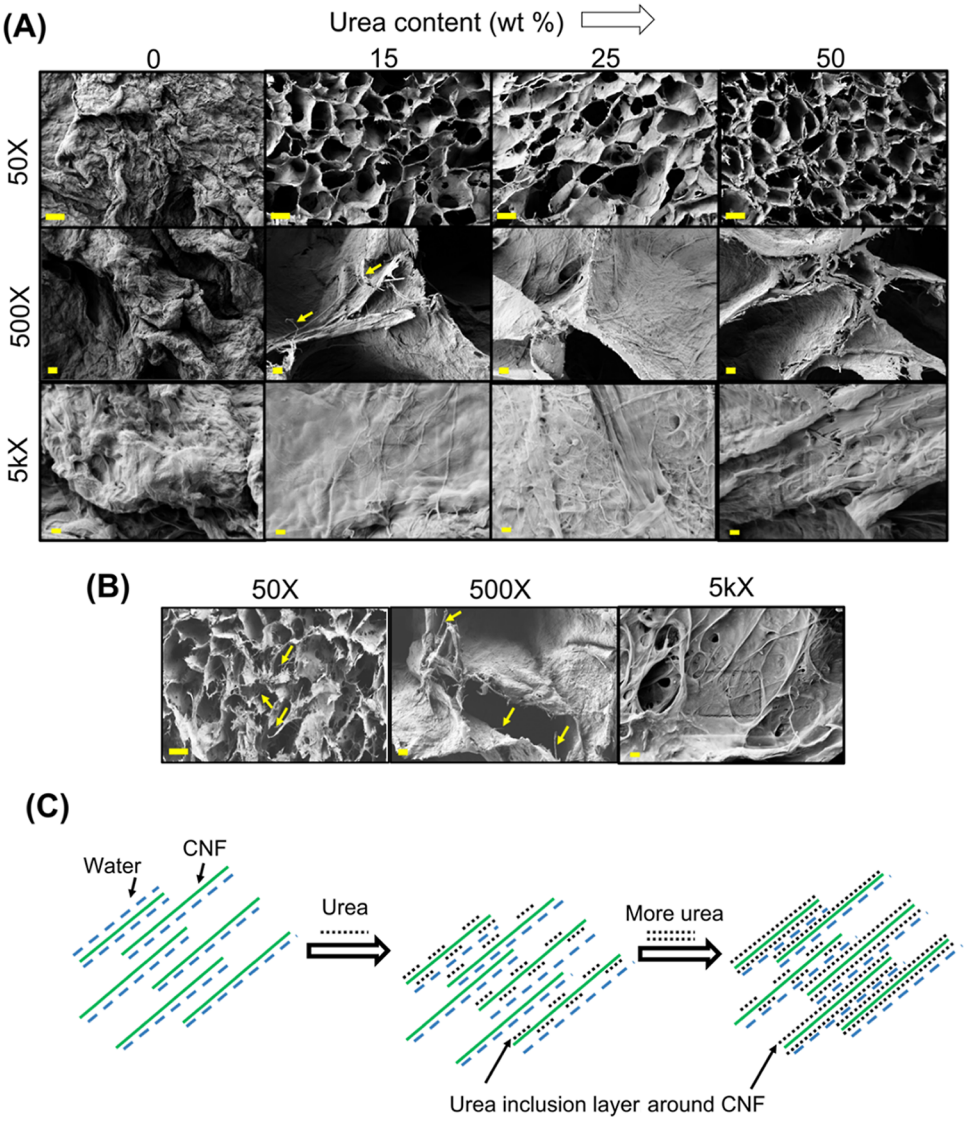

Figure 2. SEM micrographs of CNF foams without (0 wt %) and with (additional 15, 25, and 50 wt % of the dry mass of CNF) urea using MW irradiation (A) and freeze-dried CNF foams without urea of similar consistency in 50×, 500×, and 5k× magnifications (B). Scale bar at 50× is 200 μm, 500× is 10 μm, and 5k× is 1 μm. The arrows indicate the loosely hanging fibrils. Schematic representation of the effect of urea on the formation of the inclusion layer around CNF (C).

hanging fibrils is more noticeable in freeze-dried foams, which could be attributed to the lack of crosslinking among cellulose fibrils.[36]

Jiang et al.[37] investigated the interactions among NaOH, urea, and cellulose in water. Although there was no direct interaction between cellulose and urea, as demonstrated by temperature-dependent NMR data, OH^- groups in NaOH interacted with urea to create an inclusion complex with cellulose. Further addition of urea increases the inclusion complex's stability by reducing its mobility. Interestingly, at low temperatures below 25 °C, intermolecular hydrogen bonds between cellulose molecules have been demonstrated to initiate breakdown, preventing the aggregation of individual cellulose inclusion complexes.

On the other hand, Cai et al.[38] investigated the interaction between cellulose and urea in an aqueous medium in the absence of NaOH using molecular dynamics simulation. The study revealed that the stability of the inclusion layer complex between cellulose and urea depends on the minimized interaction between cellulose chains. This phenomenon is caused by the formation of hydrogen bonds between cellulose and urea molecules using the oxygen atoms of urea as proton acceptors and the hydroxyl hydrogen atoms of cellulose as proton donors. This kind of hydrogen bonding between cellulose and urea is very temperature-dependent and maintains the stability of the inclusion complex below 265 K (−8.15 °C). The study also revealed that, in a cellulose/urea/water system, almost two-thirds of the cellulose-water hydrogen bonds were replaced by cellulose-urea hydrogen bonds, allowing the formation of inclusion layers of urea around cellulose at a low temperature (Figure 2C). To verify this in our system, two additional thawing conditions were studied in addition to instantaneous thawing. The two conditions are (1) thawing at 8 °C for 24 h and (2) thawing at room temperature (~23 °C) for 24 h, both followed by the same microwave drying conditions. Figure S1A,B show that as the thawing temperature increases, the formed structures become denser.

https://doi.org/10.1021/acssuschemeng.3c00599
ACS Sustainable Chem. Eng. 2023, 11, 13240−13250

Figure S1C,D shows the effect of the freezing rate on the density and shrinkage of the UCNF foams. One-way ANOVA showed that density (35−37 kg/m^3) and volumetric shrinkage were not statistically different at different freezing rates. However, flash freezing using liquid nitrogen resulted in a collapsed and dense structure during microwave drying, which indicates that the rate of freezing might be a critical factor for forming this type of structure. Besides, when CNF suspension of similar consistency (without urea) was frozen and instantaneously thawed by microwaving, its structure collapsed, regardless of the freezing rate. This was expected given the extensive network of hydrogen bonding that forms between the fibrils. Therefore, it is reasonable to assume that additional factors might influence the formation of porous structures of CNF/urea along with the freezing rate, such as capillary forces due to the partial melting of ice crystals before the evaporation during microwave drying.

Although foams prepared at different freezing rates did not vary in their densities, the internal pore structures were different. The UCNF foam prepared at a slow freezing rate (0.06 °C/min) had a more homogeneous internal pore structure compared to foams prepared at a fast-freezing rate (0.39 °C/min) that showed a less uniform pore structure by forming large irregular voids and cracks inside (Figure 3A).

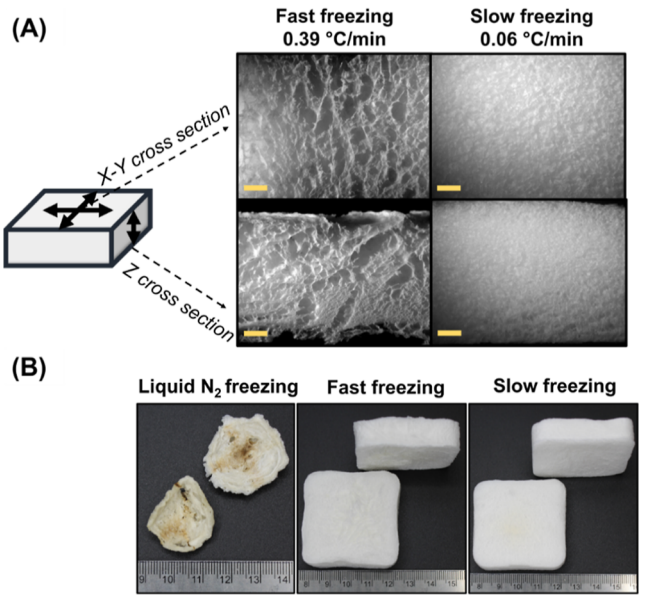

Figure 3. Variation of foam morphology observed under an optical microscope along the *X*−*Y* and *Z* directional cross sections (scale bar: 2 mm) (A) and the digital photographs of UCNF foams with different freezing rates after drying in the microwave (B). Ruler units are in cm.

The formation of distinct pore morphologies at different freezing rates may be caused by several concurrent events. Ice crystal size in a frozen sample is known to be significantly influenced by freezing temperature and rate. In this study, urea acts as the solute component of the system. It is worth noting that the difference in freezing rates of the samples themselves with and without urea under the same freezing conditions (fast freezing) was insignificant. The 2 wt % CNF suspension without urea had a freezing rate of 0.42 °C/min, whereas with 25% additional urea, the freezing rate was 0.43 °C/min. Moreover, according to the freezing point depression principle, the addition of urea to water decreases the freezing temperature to a small extent, which likely does not affect the pore size significantly.

The overall time required to freeze UCNF suspension may affect the formation of urea inclusion complexes with cellulose. On the one hand, slow freezing could allow sufficient time for the urea inclusion complex to form around individual fibrils, resulting in homogeneous pore sizes after drying. Additionally, the coalescing of ice crystals may also take place during freezing at a slow freezing rate.[39]

On the other hand, a fast-freezing rate might cause partially formed self-assembled urea inclusion complexes around the cellulose fibrils. Due to incomplete inclusion, the relative distances among those inclusion complexes might not be homogeneous which could be responsible for partial agglomeration of CNFs, resulting in large non-homogeneous pores in the sample after drying.

Finally, in the case of liquid nitrogen/flash freezing, CNFs agglomerated after microwave drying without creating a porous structure (Figure 3B). This may also be related to the ice crystal size as well as the time associated with the formation of the urea inclusion complex. It is known that liquid nitrogen freezing produces a large number of tiny crystals[40] that do not have sufficient time to coalesce compared to the conventional fast or slow freezing. Besides, due to the shortest possible freezing time, the self-assembled urea inclusion layer might not develop to the level necessary to create a porous structure. At the same time, the interfibrillar distance is significantly smaller due to the formation of tiny ice crystals, which brings the CNFs closer to each other, resulting in their agglomeration upon microwave drying. Consequently, even in the presence of urea, the intermolecular hydrogen bonding among CNFs becomes the dominating factor for agglomeration after drying the frozen suspension. The schematic of the proposed mechanism is presented in Figure 4A.

Effect of Microwave Power. Four microwave power settings (360, 600, 840, and 1200 W) were tested to examine their effect on the produced foam. Higher power results in more vigorous vibration of water molecules and, hence, faster water removal and possibly changes in the internal pore structure. At 360 W, the foams required 9 min to reach a moisture content of ∼7−10%, whereas at 1200 W, the same moisture content was reached in 4 min. The density of the foams prepared at 360 W was significantly higher (47 kg/m^3) compared to other power settings (40−42 kg/m^3). The increased density at the lowest power setting (i.e., longest drying time) indicates the critical role of thawing time in obtaining a porous structure. This finding supports the results shown in Figures S1A,B, where prolonged exposure to a higher temperature (8 and 24 °C) during thawing resulted in a dense and collapsed structure. To further support this finding, UCNF foams were prepared using oven drying and compared with those prepared by microwaving. The time required to oven dry a foam sample at 80 °C containing 97.5% of "frozen" water was 6 h, which was considerably longer than microwaving. Figure 4B shows digital photographs of UCNF foams dried in the microwave oven after different thawing times. The results show that oven drying resulted in denser and less uniform structures compared to those prepared by microwaving. Again, this verifies the importance of instant and rapid thawing/drying through microwave drying to form a uniform porous structure from urea and CNF. Finally, to examine whether continuous or non-continuous drying influences foam structure, foams were dried continuously without intervals. The results showed that

https://doi.org/10.1021/acssuschemeng.3c00599
ACS Sustainable Chem. Eng. 2023, 11, 13240−13250

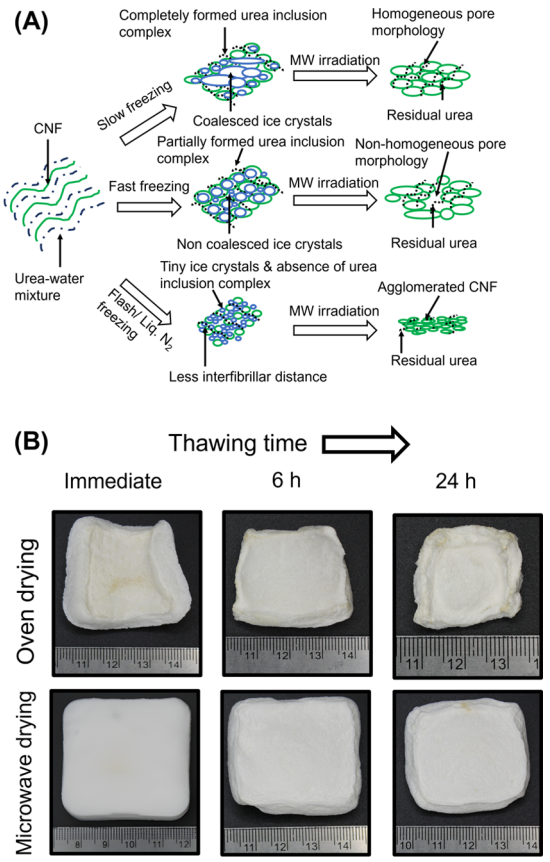

Figure 4. Proposed foam forming mechanism involving ice crystals and the urea inclusion layer with different freezing pathways (A) and the UCNF foams dried in the oven and microwave immediately after freezing and after 6 and 24 h of room temperature thawing (B).

there was no statistical difference between the two sets of samples.

Foam Stability and Crosslinking. UCNF foams showed favorable stability in wet conditions. The mass loss after soaking and agitating in water was less than 1 wt %, which suggests the possibility of a crosslinking event. It is likely that this stability is due to covalent bonding rather than weak physical interactions. To further investigate this, FTIR analysis was performed on UCNF, rinsed UCNF, and freeze-dried CNF foams (Figure 5A). The FTIR spectra of all three samples showed a broad peak around 3340 cm^{-1} and a sharp one at 2916 cm^{-1}, corresponding to −OH stretching and −CH stretching vibrations, respectively.[41] Cellulose peaks between 1650 and 900 cm^{-1} were observed, as well as a 1644 cm^{-1} peak for the adsorbed water molecule −OH group in the cellulose surface.[42] However, in the case of UCNF foam, a new peak at 1715 cm^{-1} was observed, which corresponds to the carbamate carbonyl group (C═O).[43−45] The peak at 1666 cm^{-1} is attributed to the carbonyl group of urea. To eliminate the effect of unreacted urea, the foams were rinsed with water to wash out residual urea. The small carbamate carbonyl peak of the washed sample shifted to a higher wavenumber at 1745 cm^{-1} as opposed to 1715 cm^{-1} in unwashed samples. According to the literature, the peak in this region corresponds to the carbonyl group of cellulose ester,[46,47] suggesting the formation of ester groups between urea and cellulose upon heating.

Furthermore, Figure 5B shows the solid-state ^{13}C HRMAS NMR spectra for the same three samples. The chemical shifts of carbon in the spectra could be assigned to 103.6 ppm for interior C4, 73.7 ppm for C2, C3, and C5, and 63.7 ppm for C6.[48] Apart from the peaks for cellulose, there are a few subtle differences among the three NMR spectra. The chemical shift of the C═O group for crystalline urea is at 163.4 ppm.[49] This

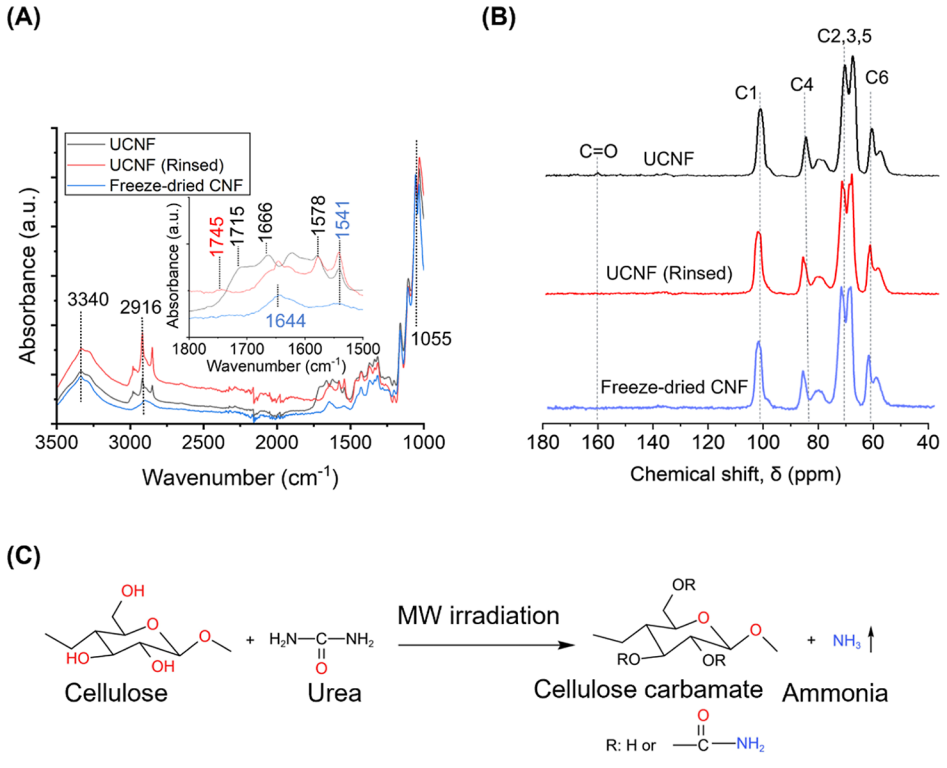

Figure 5. FTIR (A), ^{13}C HRMAS NMR (B) spectra of different CNF foams, and the possible crosslinking reaction (C).

https://doi.org/10.1021/acssuschemeng.3c00599
ACS Sustainable Chem. Eng. 2023, 11, 13240−13250

urea C═O peak shifted to 160.1 ppm due to the adsorption of urea on cellulose induced by weak hydrogen bonding.[35] However, upon rinsing with water, this peak was not observed, indicating that the peak corresponded to residual urea. Hence, it may be possible that the stability of foams in water was caused by a small amount of urea that reacted with cellulose, which was undetected by NMR and hardly detected by FTIR. Further characterization will be needed to gain insights into the wet stability of these foams.

To confirm this, the nitrogen content of foams was measured by the combustion method. The results showed that freeze-dried CNF foams contained a negligible amount of nitrogen (0.04%), likely due to impurities in the cellulose fraction. On the other hand, the nitrogen content of the UCNF foams was 3.5%, which was reduced to 1.55% after rinsing with water. Doubling the amount of rinse water resulted in a negligible loss of nitrogen content (1.34%). This result, combined with FTIR and NMR, suggests the presence of covalent bonds between cellulose and urea that likely form cellulose carbamate esters. These covalent bonds, however, were hardly detectable by FTIR and NMR due to their small concentrations. This extent of crosslinking, however, is sufficient to render the foams stable in water when mildly agitated. The resulting crosslinking is likely due to a heat-induced reaction during microwaving (Figure 5C). Previous studies also reported the formation of cellulose carbamate by heating cellulose and urea. For instance, cellulose carbamate was synthesized on cotton linters via microwave irradiation.[49,50]

In addition to the crosslinking reaction, it is important to shed light on the decomposition of urea. The mechanism of aqueous urea decomposition has long been investigated by several researchers. For example, in a relatively recent study using computational methods,[51] it was reported that urea preferentially decomposes in an aqueous medium to ammonium rather than hydrolysis due to the less required activation energy. In addition, the effect of temperature on aqueous urea decomposition was studied in an earlier work that examined the extent of urea decomposition between 60 and 100 °C[52] and the results showed a relatively small rate of urea decomposition. In the present study, the extent of urea decomposition was determined gravimetrically by measuring the mass of dry foam and comparing it with the initial dry mass. The mass difference was negligible, assuming insignificant decomposition of urea during drying.

Hybrid Foams. Hybrid foams were prepared by incorporating IONPs into the foams at various loadings. The density of the foams ranged between 31 and 45 kg/m^3 after the addition of IONPs. Hybrid foams were also tested for their stability in water under agitation. The average mass loss of the hybrid foams containing 7 wt % IONP was 10%, whereas at 3 wt % IONP mass loss was at 5.3%. However, an IONP loading of 10 wt % resulted in a significantly higher mass loss (33%).

Figure 6 shows the digital photographs and SEM images of the UCNF foams with different IONP loadings. A previous study measured the IONP-specific surface area at 162 m^2 g^{-1}.[16] Due to their hydrophilic nature and the positively charged surface under the pH condition of this study, the IONP surface forms hydrogen bonding as well as physical crosslinking with the CNF.[53] As the IONP concentration increases, they tend to form multilayered clusters. The diameter of these clusters ranged from ∼300 nm at 3 wt % to ∼2.3 μm at 10 wt % IONP, as measured from the SEM micrographs. This could explain

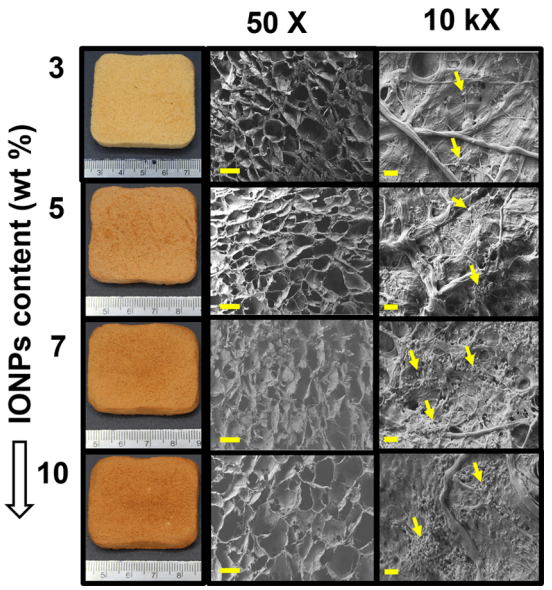

Figure 6. Digital photographs of UCNF-IONP hybrid foams with different IONP contents and the SEM images of corresponding hybrid foams in two different magnifications (50× and 10k×). The arrows indicate the cluster of IONPs. Scale bar for 50× is 100 μm and for 10k× is 1 μm.

the increased mass loss of foams containing 10 wt % IONP which results from the higher fraction of agglomerated IONPs within the foam, which disrupts the extent of carbamate crosslinking leading to the disintegration of the foam in contact with water.

Comparison of Foam Processing Procedures. Table 1 presents a comparison of the physical properties of cellulose-based foams/aerogels prepared by different procedures. Ferenczi et al.[54] investigated the power consumption of different drying techniques. The results showed that microwave vacuum drying requires almost 12 times less energy than freeze-drying. Apart from energy and time efficiency, there are several additional advantages of the foams produced by microwave irradiation in the present study. First, there is no external foaming agent such as octylamine (OA) or pluronic P123 used for this foam-forming process; such reagents have been used extensively by previous studies, especially while replacing freeze-drying or supercritical CO_2 drying with oven/convection drying.[19,20,55,56] Second, in this study, the wet stability of the foams is achieved with an in situ crosslinking reaction compared to the more complex steps reported in previous studies.[19,36,57] Overall, this study reports a simple approach to produce wet stable CNF-based foams with significant time and energy efficiency.

Mechanical Properties. Figure 7A shows compressive stress−strain curves for the UCNF foams with 25% urea and the UCNF-IONP foams with 25% urea and 3% IONPs in both wet and dry conditions performed with an experimental setup presented in Figure 7B. Freeze-dried CNF foams were also tested for comparison purposes. Those foams had a density of 26.4 kg/m^3 and were crosslinked using 5 wt % Polycup. The dry CNF and UCNF foams showed three regions for a typical foam compressive stress−strain curve: a linear elastic region, a stress plateau region, and a densification region.[65] The compressive stress of the dry foams increased gradually up to 65% and rapidly afterward (densification region). Although the compressive modulus of the dry foams was not statistically

https://doi.org/10.1021/acssuschemeng.3c00599
ACS Sustainable Chem. Eng. 2023, 11, 13240−13250

Table 1. Comparison among Cellulose-Based Foams/Aerogel Processing Procedures[a]

nanocellulose type	reagents	processing technique	drying technique and time	density (kg/m^3)	porosity (%)	stability in water	reference
TEMPO-CNF		FC	FD	5.6	99.6		58
CMCNF	OA	high-speed mixing	OD	9−109	92.7−99.4		20
TEMPO-CNF	OA and SMP	high-speed mixing	OD	6−200	87−99.6	hydrophilic and stable	19
TEMPO-CNF	pluronic P123, $CaCO_3$, and GDL	high-speed mixing	CD	9.6−15.2			56
CMCNa	PEGDA and pluronic F-127	high-speed mixing	MWC and VD				55
CNF	EtOH, 2-propanol, and PVA	freezing with dry ice and EtOH	SE and AD	18	>98		59
MFC	urea	controlled freezing	AD (48 h) and OD (18 h)	29.1−36.4	97.4−98.1		21
CNF		liquid N_2 freezing (10 s) or conventional freezing (24 h)	$ScCO_2$ drying	9−50	96.9−99.4		60
CNF	TiO_2	freezing and ALD	FD	20−30	>98	hydrophobic	61
TEMPO-CNF	EtOH and tBuOH	SE	$ScCO_2$ and FD	24.3		unstable	62
NFC	TMCS	freezing and VPD	FD	3.12		hydrophobic	63
NFC	PVA	freezing (6 h)	FD (48 h)	7−20	99.51−98.52	hydrophobic	64
CNF	MetCMC	UV-radiation followed by freezing in liquid N_2	FD	87.5	95	stable	57
CNF	urea	conventional freezing	MW (7 min)	35−37	>97	stable	this work
CNF	urea and IONPs	conventional freezing	MW (7 min)	37−38	>97	stable	this work

[a]Abbreviations: TEMPO: 2,2,6,6-tetramethylpiperidine-1-oxyl radical, CMCNFs: carboxymethyl cellulose nanofibrils, OA: octylamine, SMP: sodium (meta)periodate, pluronic P123: pluronic tri-block (EO-PO-EO) copolymer P123, GDL: D-(+)-gluconic acid D-lactone, CMCNa: a sodium salt of carboxymethylcellulose, PEGDA: polyethylene glycol diacrylate, PVA: poly(vinyl alcohol), TMCS: trimethylchlorosilane, NFC: nanofibrillated cellulose, VPD: vapor phase deposition, MetCMC: methacrylate functionalized carboxymethyl cellulose, FC: freeze casting, FD: freeze-drying, OD: oven-drying, CD: convection-drying, MWC: microwave curing, VD: vacuum drying, AD: ambient-drying, SE: solvent exchange, $ScCO_2$ drying: supercritical CO_2 drying, TiO_2: titanium dioxide, $CaCO_3$: calcium carbonate, ALD: atomic layer deposition, MFC: microfibrillated cellulose, EtOH: ethanol, *t*BuOH: *tert*-butyl alcohol, and MW: microwave irradiation.

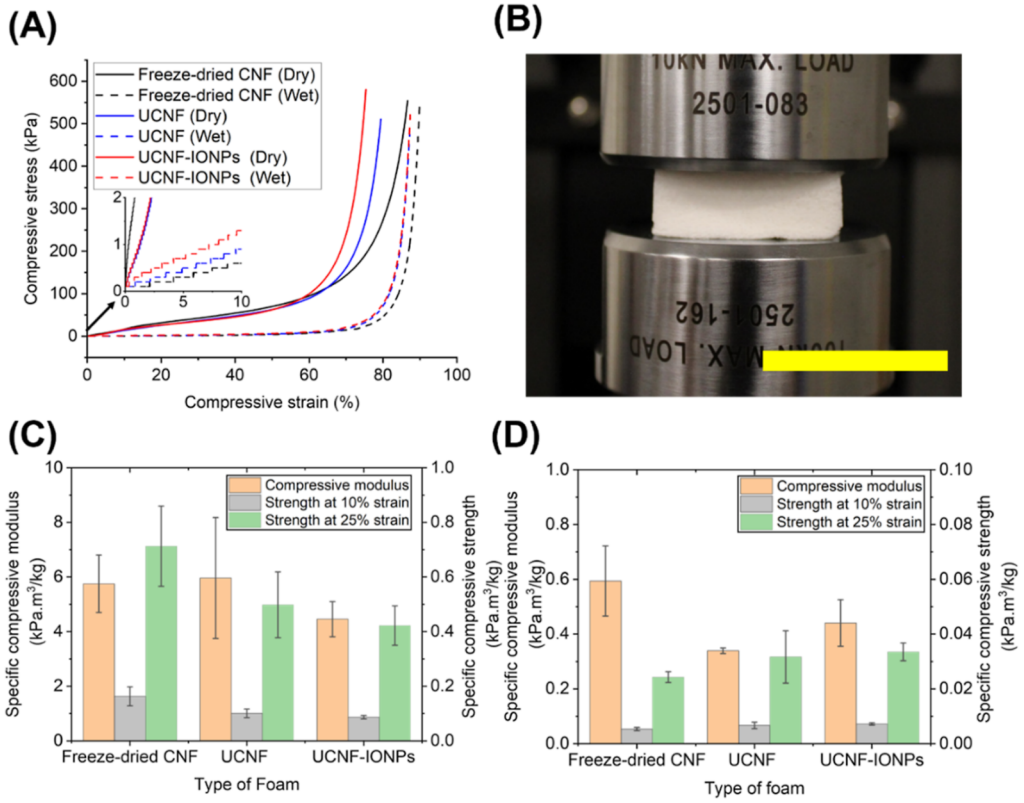

Figure 7. Stress−strain curves for both dry and wet foams (A), photo of the experimental setup (scale bar is 3 cm) (B), and specific compressive modulus and compressive strength at 10 and 25% strain for dry (C) and wet (D) foams. The error bars represent one standard deviation among three replicates for each group.

https://doi.org/10.1021/acssuschemeng.3c00599
ACS Sustainable Chem. Eng. 2023, 11, 13240−13250

different, the compressive strengths were different (Figure 7C). Freeze-dried CNF foams showed slightly higher compressive strengths compared to the UCNF foams at similar strain levels. It is worth mentioning that the compressive moduli and strengths at both 10 and 25% strain levels for UCNF foams did not show any statistical difference from the UCNF-IONP foam. Also, the UCNF foams showed a lower compressive modulus compared to the previous urea-based foams[21,34] at around similar densities. However, the urea content of those foams was four times higher than that of the UCNF or UCNF-IONP foams in this study.

The increased mechanical properties of foams in previous studies[21,34] may be caused by factors other than their higher urea content, such as their varied supply of raw materials or testing conditions. On the other hand, all the wet foams showed a considerable drop in both compressive moduli and strengths (Figure 7D) compared to dry samples. The freeze-dried CNF foams had a statistically higher specific compressive modulus than the UCNF and UCNF-IONP foams. The specific compressive strength of the wet freeze-dried foam at 10% strain was not statistically different from the wet UCNF and UCNF-IONP foams. But at 25% strain, the wet freeze-dried foam showed a statistically lower compressive strength than the wet UCNF-based foams. Overall, the mechanical performance of foams produced by the microwave-assisted method is comparable to that produced by freeze-drying. A summary of the compressive testing results is presented in Table S1.

CONCLUSIONS

Freezing followed by instantaneous thawing−drying of a UCNF produced low-density (36 kg/m^3) CNF foams. A 15 wt % urea content was sufficient to produce these foams, which is significantly less than what was used in prior research. Instantaneous thawing has been identified as a crucial factor in the production of CNF foams with low density and limited shrinkage. The microscopic images revealed that the foams formed at a slow freezing rate had pores with a uniform shape. Intriguingly, fast freezing in a freezing chamber or with liquid nitrogen resulted in either the formation of voids in the foam structure or total CNF agglomeration. Due to the presence of heat-induced in situ carbamate crosslinking, the foams exhibited a favorable degree of stability in water. This feature was not altered by the hybridization of the CNF foams with IONPs. This study demonstrates the potential for large-scale, continuous manufacturing of nanocellulose-based porous foams at a lower cost and with lower energy consumption than any previously reported methods, thereby enhancing the viability of this porous material as a component of widely available commercial products.

ASSOCIATED CONTENT

Supporting Information

The Supporting Information is available free of charge at https://pubs.acs.org/doi/10.1021/acssuschemeng.3c00599.

Additional experimental details of the measurements of density, porosity, and shrinkage of the foams, statistical analysis, and compressive testing; results of density and shrinkage of the foams; and summary of compressive properties results (PDF)

AUTHOR INFORMATION

Corresponding Author

Islam Hafez − *Department of Wood Science and Engineering, Oregon State University, Corvallis, Oregon 97331, United States;* orcid.org/0000-0002-7450-4135; Email: islam.hafez@oregonstate.edu

Authors

Md Musfiqur Rahman − *Laboratory of Renewable Nanomaterials, School of Forest Resources, University of Maine, Orono, Maine 04469, United States;* orcid.org/0000-0003-0884-6847

Mehdi Tajvidi − *Laboratory of Renewable Nanomaterials, School of Forest Resources, University of Maine, Orono, Maine 04469, United States;* orcid.org/0000-0002-3549-1220

Aria Amirbahman − *Department of Civil, Environmental and Sustainable Engineering, Santa Clara University, Santa Clara, California 95053, United States*

Complete contact information is available at: https://pubs.acs.org/10.1021/acssuschemeng.3c00599

Author Contributions

The manuscript was written through the contributions of all authors. All the authors have given approval to the final version of the manuscript.

Notes

The authors declare no competing financial interest.

ACKNOWLEDGMENTS

This work is financially supported by the United States Department of Agriculture (USDA) Forest Services. The authors would like to acknowledge GlycoMIP, a National Science Foundation Materials Platform funded through Cooperative Agreement DMR-1933525 for the ^{13}C NMR data.

REFERENCES

(1) Moon, R. J.; Martini, A.; Nairn, J.; Simonsen, J.; Youngblood, J. Cellulose Nanomaterials Review: Structure, Properties and Nanocomposites. *Chem. Soc. Rev.* **2011**, *40*, 3941.

(2) Phanthong, P.; Reubroycharoen, P.; Hao, X.; Xu, G.; Abudula, A.; Guan, G. Nanocellulose: Extraction and Application. *Carbon Resour. Convers.* **2018**, *1*, 32−43.

(3) Trache, D.; Tarchoun, A. F.; Derradji, M.; Hamidon, T. S.; Masruchin, N.; Brosse, N.; Hussin, M. H. Nanocellulose: From Fundamentals to Advanced Applications. *Front. Chem.* **2020**, *8*, 392.

(4) Chen, C.; Sun, W.; Wang, L.; Tajvidi, M.; Wang, J.; Gardner, D. J. Transparent Multifunctional Cellulose Nanocrystal Films Prepared Using Trivalent Metal Ion Exchange for Food Packaging. *ACS Sustain. Chem. Eng.* **2022**, *10*, 9419−9430.

(5) Hasan, I.; Wang, J.; Tajvidi, M. Tuning Physical, Mechanical and Barrier Properties of Cellulose Nanofibril Films through Film Drying Techniques Coupled with Thermal Compression. *Cellulose* **2021**, *28*, 11345−11366.

(6) Hossain, R.; Tajvidi, M.; Bousfield, D.; Gardner, D. J. Recyclable Grease-Proof Cellulose Nanocomposites with Enhanced Water Resistance for Food Serving Applications. *Cellulose* **2022**, *29*, 5623−5643.

(7) Li, L.; Maddalena, L.; Nishiyama, Y.; Carosio, F.; Ogawa, Y.; Berglund, L. A. Recyclable Nanocomposites of Well-Dispersed 2D Layered Silicates in Cellulose Nanofibril (CNF) Matrix. *Carbohydr. Polym.* **2022**, *279*, 119004.

(8) Chen, C.; Hu, L. Nanocellulose toward Advanced Energy Storage Devices: Structure and Electrochemistry. *Acc. Chem. Res.* **2018**, *51*, 3154−3165.

(9) Jorfi, M.; Foster, E. J. Recent Advances in Nanocellulose for Biomedical Applications. *J. Appl. Polym. Sci.* **2015**, *132*, 41719.
(10) LakshmiBalasubramaniam, S.; Patel, A. S.; Nayak, B.; Howell, C.; Skonberg, D. Antioxidant and Antimicrobial Modified Cellulose Nanofibers for Food Applications. *Food Biosci.* **2021**, *44*, 101421.
(11) Voisin, H.; Bergström, L.; Liu, P.; Mathew, A. Nanocellulose-Based Materials for Water Purification. *Nanomaterials* **2017**, *7*, 57.
(12) Nechita, P.; Năstac, S. M. Overview on Foam Forming Cellulose Materials for Cushioning Packaging Applications. *Polymers* **2022**, *14*, 1963.
(13) Jiang, S.; Zhang, M.; Li, M.; Zhu, J.; Ge, A.; Liu, L.; Yu, J. Cellulose-Based Composite Thermal-Insulating Foams toward Eco-Friendly, Flexible and Flame-Retardant. *Carbohydr. Polym.* **2021**, *273*, 118544.
(14) Abdelhamid, H. N.; Mathew, A. P. Cellulose-Based Materials for Water Remediation: Adsorption, Catalysis, and Antifouling. *Front. Chem. Eng.* **2021**, *3*, 790314.
(15) da Silva, D. J.; Rosa, D. S. Chromium Removal Capability, Water Resistance and Mechanical Behavior of Foams Based on Cellulose Nanofibrils with Citric Acid. *Polymer* **2022**, *253*, 125023.
(16) Rahman, M. M.; Hafez, I.; Tajvidi, M.; Amirbahman, A. Highly Efficient Iron Oxide Nanoparticles Immobilized on Cellulose Nanofibril Aerogels for Arsenic Removal from Water. *Nanomaterials* **2021**, *11*, 2818.
(17) Zhu, H.; Yang, X.; Cranston, E. D.; Zhu, S. Flexible and Porous Nanocellulose Aerogels with High Loadings of Metal-Organic-Framework Particles for Separations Applications. *Adv. Mater.* **2016**, *28*, 7652−7657.
(18) Lavoine, N.; Bergström, L. Nanocellulose-Based Foams and Aerogels: Processing, Properties, and Applications. *J. Mater. Chem. A* **2017**, *5*, 16105−16117.
(19) Cervin, N. T.; Johansson, E.; Larsson, P. A.; Wågberg, L. Strong, Water-Durable, and Wet-Resilient Cellulose Nanofibril-Stabilized Foams from Oven Drying. *ACS Appl. Mater. Interfaces* **2016**, *8*, 11682−11689.
(20) Park, S. Y.; Goo, S.; Shin, H.; Kim, J.; Youn, H. J. Structural Properties of Cellulose Nanofibril Foam Depending on Wet Foaming Conditions in Pickering Stabilization. *Cellulose* **2021**, *28*, 10291−10304.
(21) Josset, S.; Hansen, L.; Orsolini, P.; Griffa, M.; Kuzior, O.; Weisse, B.; Zimmermann, T.; Geiger, T. Microfibrillated Cellulose Foams Obtained by a Straightforward Freeze−Thawing−Drying Procedure. *Cellulose* **2017**, *24*, 3825−3842.
(22) Cai, J.; Zhang, L. Rapid Dissolution of Cellulose in LiOH/Urea and NaOH/Urea Aqueous Solutions. *Macromol. Biosci.* **2005**, *5*, 539−548.
(23) Fauziyah, M.; Widiyastuti, W.; Balgis, R.; Setyawan, H. Production of Cellulose Aerogels from Coir Fibers via an Alkali−Urea Method for Sorption Applications. *Cellulose* **2019**, *26*, 9583−9598.
(24) Hafez, I.; Tajvidi, M. Comprehensive Insight into Foams Made of Thermomechanical Pulp Fibers and Cellulose Nanofibrils via Microwave Radiation. *ACS Sustain. Chem. Eng.* **2021**, *9*, 10113−10122.
(25) Tauhiduzzaman, M.; Hafez, I.; Bousfield, D.; Tajvidi, M. Modeling Microwave Heating and Drying of Lignocellulosic Foams through Coupled Electromagnetic and Heat Transfer Analysis. *Processes* **2021**, *9*, 2001.
(26) Nirmaan, A. M. C.; Rohitha Prasantha, B. D.; Peiris, B. L. Comparison of Microwave Drying and Oven-Drying Techniques for Moisture Determination of Three Paddy (Oryza Sativa L.) Varieties. *Chem. Biol. Technol. Agric.* **2020**, *7*, 1.
(27) Sun, J.; Wang, W.; Yue, Q. Review on Microwave-Matter Interaction Fundamentals and Efficient Microwave-Associated Heating Strategies. *Materials* **2016**, *9*, 231.
(28) Anwar, J.; Shafique, U.; Waheed-uz-Zaman; Rehman, R.; Salman, M.; Dar, A.; Anzano, J. M.; Ashraf, U.; Ashraf, S. Microwave Chemistry: Effect of Ions on Dielectric Heating in Microwave Ovens. *Arab. J. Chem.* **2015**, *8*, 100−104.
(29) Mingos, D. M. P.; Baghurst, D. R. Tilden Lecture. Applications of microwave dielectric heating effects to synthetic problems in chemistry. *Chem. Soc. Rev.* **1991**, *20*, 1.
(30) Wang, D.; Feng, X.; Zhang, L.; Li, M.; Liu, M.; Tian, A.; Fu, S. Cyclotriphosphazene-Bridged Periodic Mesoporous Organosilica-Integrated Cellulose Nanofiber Anisotropic Foam with Highly Flame-Retardant and Thermally Insulating Properties. *Chem. Eng. J.* **2019**, *375*, 121933.
(31) Rabani, I.; Yoo, J.; Kim, H.-S.; Lam, D. V.; Hussain, S.; Karuppasamy, K.; Seo, Y.-S. Highly Dispersive Co_3O_4 Nanoparticles Incorporated into a Cellulose Nanofiber for a High-Performance Flexible Supercapacitor. *Nanoscale* **2021**, *13*, 355−370.
(32) Salahuddin, B.; Aziz, S.; Gao, S.; Hossain, M. S. A.; Billah, M.; Zhu, Z.; Amiralian, N. Magnetic Hydrogel Composite for Wastewater Treatment. *Polymers* **2022**, *14*, 5074.
(33) Zhang, W.; Zhang, Y.; Lu, C.; Deng, Y. Aerogels from Crosslinked Cellulose Nano/Micro-Fibrils and Their Fast Shape Recovery Property in Water. *J. Mater. Chem.* **2012**, *22*, 11642.
(34) Antonini, C.; Wu, T.; Zimmermann, T.; Kherbeche, A.; Thoraval, M.-J.; Nyström, G.; Geiger, T. Ultra-Porous Nanocellulose Foams: A Facile and Scalable Fabrication Approach. *Nanomaterials* **2019**, *9*, 1142.
(35) Holm Kristensen, J.; Bampos, N.; Duer, M. Solid State 13C CP MAS NMR Study of Molecular Motions and Interactions of Urea Adsorbed on Cotton Cellulose. *Phys. Chem. Chem. Phys.* **2004**, *6*, 3175.
(36) González-Ugarte, A. S.; Hafez, I.; Tajvidi, M. Characterization and Properties of Hybrid Foams from Nanocellulose and Kaolin-Microfibrillated Cellulose Composite. *Sci. Rep.* **2020**, *10*, 17459.
(37) Jiang, Z.; Fang, Y.; Xiang, J.; Ma, Y.; Lu, A.; Kang, H.; Huang, Y.; Guo, H.; Liu, R.; Zhang, L. Intermolecular Interactions and 3D Structure in Cellulose−NaOH−Urea Aqueous System. *J. Phys. Chem. B* **2014**, *118*, 10250−10257.
(38) Cai, L.; Liu, Y.; Liang, H. Impact of Hydrogen Bonding on Inclusion Layer of Urea to Cellulose: Study of Molecular Dynamics Simulation. *Polymer* **2012**, *53*, 1124−1130.
(39) Regand, A.; Goff, H. D. Structure and Ice Recrystallization in Frozen Stabilized Ice Cream Model Systems. *Food Hydrocolloids* **2003**, *17*, 95−102.
(40) Zhang, M.; Li, M.; Xu, Q.; Jiang, W.; Hou, M.; Guo, L.; Wang, N.; Zhao, Y.; Liu, L. Nanocellulose-Based Aerogels with Devisable Structure and Tunable Properties via Ice-Template Induced Self-Assembly. *Ind. Crops Prod.* **2022**, *179*, 114701.
(41) Hospodarova, V.; Singovszka, E.; Stevulova, N. Characterization of Cellulosic Fibers by FTIR Spectroscopy for Their Further Implementation to Building Materials. *Am. J. Anal. Chem.* **2018**, *09*, 303−310.
(42) Poletto, M.; Pistor, V.; Zeni, M.; Zattera, A. J. Crystalline Properties and Decomposition Kinetics of Cellulose Fibers in Wood Pulp Obtained by Two Pulping Processes. *Polym. Degrad. Stab.* **2011**, *96*, 679−685.
(43) Segal, L.; Eggerton, F. V. Some Aspects of the Reaction between Urea and Cellulose. *Text. Res. J.* **1961**, *31*, 460−471.
(44) Willberg-Keyriläinen, P.; Hiltunen, J.; Ropponen, J. Production of Cellulose Carbamate Using Urea-Based Deep Eutectic Solvents. *Cellulose* **2018**, *25*, 195−204.
(45) Xiong, L.-K.; Yu, G.-M.; Yin, C.-Y. Synthesis and Characterization of Cellulose Carbamate by Liquid-Solid Phase Method. *Fibers Polym.* **2017**, *18*, 88−94.
(46) Fei, P.; Liao, L.; Cheng, B.; Song, J. Quantitative Analysis of Cellulose Acetate with a High Degree of Substitution by FTIR and Its Application. *Anal. Methods* **2017**, *9*, 6194−6201.
(47) Jandura, P.; Kokta, B. V.; Riedl, B. Fibrous Long-Chain Organic Acid Cellulose Esters and Their Characterization by Diffuse Reflectance FTIR Spectroscopy, Solid-State CP/MAS13C-NMR, and X-Ray Diffraction. *J. Appl. Polym. Sci.* **2000**, *78*, 1354−1365.
(48) Isogai, A.; Usuda, M.; Kato, T.; Uryu, T.; Atalla, R. H. Solid-State CP/MAS Carbon-13 NMR Study of Cellulose Polymorphs. *Macromolecules* **1989**, *22*, 3168−3172.

https://doi.org/10.1021/acssuschemeng.3c00599
ACS Sustainable Chem. Eng. 2023, 11, 13240−13250

(49) Guo, Y.; Zhou, J.; Song, Y.; Zhang, L. An Efficient and Environmentally Friendly Method for the Synthesis of Cellulose Carbamate by Microwave Heating: An Efficient and Environmentally Friendly Method for. *Macromol. Rapid Commun.* **2009**, *30*, 1504−1508.
(50) Guo, Y.; Zhou, J.; Wang, Y.; Zhang, L.; Lin, X. An Efficient Transformation of Cellulose into Cellulose Carbamates Assisted by Microwave Irradiation. *Cellulose* **2010**, *17*, 1115−1125.
(51) Alexandrova, A. N.; Jorgensen, W. L. Why Urea Eliminates Ammonia Rather than Hydrolyzes in Aqueous Solution. *J. Phys. Chem. B* **2007**, *111*, 720−730.
(52) Shaw, W. H. R.; Bordeaux, J. J. The Decomposition of Urea in Aqueous Media. *J. Am. Chem. Soc.* **1955**, *77*, 4729−4733.
(53) Dang, B.; Chen, Y.; Wang, H.; Chen, B.; Jin, C.; Sun, Q. Preparation of High Mechanical Performance Nano-Fe3O4/Wood Fiber Binderless Composite Boards for Electromagnetic Absorption via a Facile and Green Method. *Nanomaterials* **2018**, *8*, 52.
(54) Ferenczi, S.; Molnár, H.; Adányi, N.; Cserhalmi, Z. *Comparison of Microwave Vacuum-, Eze- and Hot-Air Drying by Energy Efficiency and Aroma Composition of Dried Hop (Humulus Lupulus)*; NARIC Food Science Research Institute, 2018.
(55) Demitri, C.; Giuri, A.; Raucci, M. G.; Giugliano, D.; Madaghiele, M.; Sannino, A.; Ambrosio, L. Preparation and Characterization of Cellulose-Based Foams via Microwave Curing. *Interface Focus* **2014**, *4*, 20130053.
(56) Gordeyeva, K. S.; Fall, A. B.; Hall, S.; Wicklein, B.; Bergström, L. Stabilizing Nanocellulose-Nonionic Surfactant Composite Foams by Delayed Ca-Induced Gelation. *J. Colloid Interface Sci.* **2016**, *472*, 44−51.
(57) Hossen, M. R.; Dadoo, N.; Holomakoff, D. G.; Co, A.; Gramlich, W. M.; Mason, M. D. Wet Stable and Mechanically Robust Cellulose Nanofibrils (CNF) Based Hydrogel. *Polymer* **2018**, *151*, 231−241.
(58) Wicklein, B.; Kocjan, A.; Salazar-Alvarez, G.; Carosio, F.; Camino, G.; Antonietti, M.; Bergström, L. Thermally Insulating and Fire-Retardant Lightweight Anisotropic Foams Based on Nanocellulose and Graphene Oxide. *Nat. Nanotechnol.* **2015**, *10*, 277−283.
(59) Li, Y.; Tanna, V. A.; Zhou, Y.; Winter, H. H.; Watkins, J. J.; Carter, K. R. Nanocellulose Aerogels Inspired by Frozen Tofu. *ACS Sustain. Chem. Eng.* **2017**, *5*, 6387−6391.
(60) Ciftci, D.; Ubeyitogullari, A.; Huerta, R. R.; Ciftci, O. N.; Flores, R. A.; Saldaña, M. D. A. Lupin Hull Cellulose Nanofiber Aerogel Preparation by Supercritical CO 2 and Freeze Drying. *J. Supercrit. Fluids* **2017**, *127*, 137−145.
(61) Korhonen, J. T.; Kettunen, M.; Ras, R. H. A.; Ikkala, O. Hydrophobic Nanocellulose Aerogels as Floating, Sustainable, Reusable, and Recyclable Oil Absorbents. *ACS Appl. Mater. Interfaces* **2011**, *3*, 1813−1816.
(62) Darpentigny, C.; Nonglaton, G.; Bras, J.; Jean, B. Highly Absorbent Cellulose Nanofibrils Aerogels Prepared by Supercritical Drying. *Carbohydr. Polym.* **2020**, *229*, 115560.
(63) Xiao, S.; Gao, R.; Lu, Y.; Li, J.; Sun, Q. Fabrication and Characterization of Nanofibrillated Cellulose and Its Aerogels from Natural Pine Needles. *Carbohydr. Polym.* **2015**, *119*, 202−209.
(64) Chhajed, M.; Yadav, C.; Agrawal, A. K.; Maji, P. K. Esterified Superhydrophobic Nanofibrillated Cellulose Based Aerogel for Oil Spill Treatment. *Carbohydr. Polym.* **2019**, *226*, 115286.
(65) Gibson, L. J.; Ashby, M. F. *Cellular Solids: Structure and Properties*, 2nd ed.; Cambridge University Press, 1997.

https://doi.org/10.1021/acssuschemeng.3c00599
ACS Sustainable Chem. Eng. 2023, 11, 13240−13250